Temperature and pH sensitivity of the O_{640} intermediate of the bacteriorhodopsin photocycle

I. Chizhov,* M. Engelhard,‡ D. S. Chernavskii,§ B. Zubov,* and B. Hess‡
*General Physics Institute of the Academy of Sciences, USSR, 117942 Moscow, Union of Soviet Socialist Republics;
‡Max-Planck-Institut für Ernährungsphysiologie, W-Dortmund, Germany; and §Physical Institute of the Academy of Sciences,
USSR, 117333 Moscow, Union of Soviet Socialist Republics

ABSTRACT The temperature and pH dependencies of the O_{640} intermediate of the photocycle of bacteriorhodopsin (bR) were investigated by flash photolysis and T-jump experiments. The maximal concentration of the O_{640} intermediate was found to be dependent on the temperature, which is described by a sigmoidal relationship. With increasing pH the midpoint of the sigmoidal curves shifts to higher temperatures. The Van't Hoff equation provides enthalpy and entropy values of the observed states. These results indicate that, in the investigated temperature (0–60°C) and pH (pH 4.0–10.0) range, the sequence of the principal intermediates in the pathway "M-N-O-bR" does not change. The observations of the O_{640} intermediate at pH < 8.0 and of the N_{550} intermediate at pH > 8.0 are most probably due only to changes of the intrinsic rate constants of the bR photocycle, not to a different mechanism.

1. INTRODUCTION

Bacteriorhodopsin (bR) is a membrane protein from *Halobacterium halobium* that acts as a photoactivated proton carrier in bacterial cells (for recent reviews, see references 1–4). After absorption of a light quantum ($\lambda_{max} = 570$ nm), the chromophore of bR relaxes within a few milliseconds back to the initial ground state. The intermediates of this photocycle are characterized not only by their particular absorption spectra and lifetimes but also by the isomerization and protonation state of the retinal chromophore and the protonation states of internal aspartic acid residues.

An important problem in the investigation of the mechanism of the intramolecular proton pump of bR is the elucidation of the photocycle, i.e., the number of intermediates, their spectra, and their kinetic couplings. A linear sequential model of the photocycle had first been suggested (5, 6). This scheme included five intermediates: K_{610}, L_{550}, M_{410}, N_{550}, and O_{640}, where the subscripts indicate the absorption maxima of the corresponding intermediates. Further studies on the photocycle showed that the relaxation pathway is more complicated. In particular, the last part of the photocycle, including the decay of the M intermediate and the reformation of the bR ground state, could not be described by the simple linear scheme. Sherman et al. (7) suggested a branching model of the photocycle after M_{410} in order to explain the temperature dependence of the transient concentration of the O_{640} intermediate. A biphasic decay of M was also observed (8–10). An observation (at certain conditions) of even three exponential components in the decay of the M_{410} intermediate was explained by introducing three parallel pathways of relaxation (11). An alternative explanation for these kinetic properties was proposed by Parodi et al. (12), who assumed a back reaction from O_{640} to M_{410}. This model could resolve the problem of the biphasic decay of M_{410}. However, the problem of the temperature dependence of the spectrum of the O_{640} intermediate remained.

Further experiments using temperature–pulse perturbation techniques provided evidence that an additional intermediate, the so-called N_{550} intermediate, has to be placed between M_{410} and O_{640} (13). An N_{550}-like intermediate was already proposed by Lozier et al. (6). An intermediate with similar properties was discussed in references 14 and 15. In a recent publication, Kouyama et al. (16) described the spectroscopic properties of the N_{550} intermediate at high pH. Under similar conditions Fodor et al. (17) were able to assign the chromophore structure.

Chernavskii et al. (13) explained the temperature effects of the O_{640} intermediate by assuming two consecutive reversible steps in the relaxation pathway: $M_{410} \Leftrightarrow N_{550}$ and $N_{550} \Leftrightarrow O_{640}$. This model accounts for the biphasic decay of the M_{410} intermediate by the back reaction from N_{550} to M_{410} and for the temperature dependence of the O_{640} intermediate by a quasiequilibrium between N_{550} and O_{640}. In this frame, the elusiveness of the N_{550} intermediate at ambient temperature and neutral pH can be explained because it is kinetically and spectroscopically hidden.

It is generally accepted that the reaction from M_{410} to bR goes via the N_{550} intermediate. However, it is not clear at which steps back reactions have to be assumed, and it is also not clear whether additional intermediates

0006-3495/92/04/1001/06 $2.00

like M_{410} or N_{550} are present in the photocycle (18, 19). Further insight into this part of the photocycle is expected from temperature studies of the transient concentration of the O_{640} intermediate at different pHs. Results presented in this work show that the O_{640} intermediate exists in the whole pH range studied (pH 4–10). At high pH, the transient concentration of the O_{640} intermediate is extremely low and can be detected only by raising the temperature. The pH and temperature sensitivity of the O_{640} intermediate displays a sigmoidal behavior from which thermodynamic data can be extracted and from which conclusions on the sequential nature of the overall mechanism can be drawn.

2. MATERIALS AND METHODS

Purple membranes were isolated from *H. halobium* (strain S9) as described in reference 20. For the measurements of the temperature dependence, a suspension of light-adapted bR (OD 0.7) in 12.5 mM phosphate buffer was placed into a quartz cuvette. For the T-jump experiments, 100 mM sodium chloride was added to the suspension. The pH was adjusted by using appropriate phosphate buffer between pH 4 and 8 and borate buffer for pH > 8. The cuvette geometry was $1 \times 1 \times 1\ \mathrm{cm}^3$.

The bR photocycle was initiated by a 20-ns, 532-nm, 20-mJ/cm^2 actinic pulse from a frequency-doubled neodymium yttrium aluminum garnet laser (Quantel, Orfay, France). Measuring light from a continuous halogen lamp (150 W) passed successively through an interference filter, sample, another interference filter, and then to the photodiode. For the T-jump experiments, a linear polarizer was placed into the measuring light pathway to compensate for the anisotropic effects associated with the orientation of purple membrane sheets in an external electrical field. The absorption kinetic was registered by a digital oscilloscope (Explorer; Nicolet Instrument Corp., Madison, WI). The data were stored on floppy disks or were recorded on a plotter. The wavelengths of the measuring light were 405 nm (indicative for the M_{410} intermediate), 570 nm (bR recovery), and 675 nm (formation and decay of O_{640}). The temperature was varied from 0 to 60°C using a thermostat. The state of light–dark adaptation was checked at each temperature and pH by the differential amplitude at 410 nm. Between the light- and dark-adapted samples, the amplitude changed by a factor of approximately two.

The T-jump experiments were performed by a 40-μs electrical discharge across the sample of 28 kV/cm accumulated on an external capacitor (170 nF) (for details see reference 21). It is important to note that a discharge time of 40 μs is long enough for the formation of double ion layers near the electrodes. For this reason the voltage drop across the sample is strongly nonlinear, and the actual heating of the center of the sample volume (through which the measuring light passes) differs considerably from calculations based on a homogeneous energy distribution released by the external capacitor. The half-life time of the M_{410} decay ($\tau_{1/2}$) can serve as an internal control of the actual temperature after a T-jump. For example, comparison of the kinetics accelerated by a T-jump (Fig. 1 *b*) with the kinetics from control temperatures provides a measure for the T-jump amplitude. In Fig. 1 *b* the initial temperature of the sample is 10 ± 0.5°C and $\tau_{1/2}$ is 17 ± 1 ms; after applying a T-jump $\tau_{1/2}$ accelerates to 7 ± 0.5 ms, which corresponds to a temperature of 17.5 ± 0.5°C. The actual temperature increase in the sample is, therefore, $T = 7.5 \pm 0.7$°C. On the other hand, a calculation T by the equation $\Delta T\infty = C \times U^2/2c$ (22), where C is the electrical capacity, U the voltage, and c the thermocapacity of the sample, gives a value of ~ 15°C. A more detailed analysis of this discrepancy will be published elsewhere.

3. RESULTS AND DISCUSSION

The transient concentration of the O_{640} intermediate in the photocycle after a laser pulse corresponds to the maximal differential transmittance at 675 nm (O_{max}, Fig. 1 *a*). This assumption is based on the observation that the ratio between apparent time constants of formation and decay of the O_{640} intermediate is practically temperature independent (7); hence, the temperature dependence of the O_{640} maximum reflects the dependence of the transient concentration of the O_{640} intermediate, which is illustrated in the transmittance record of Fig. 1 *a*. The traces were obtained after addi-

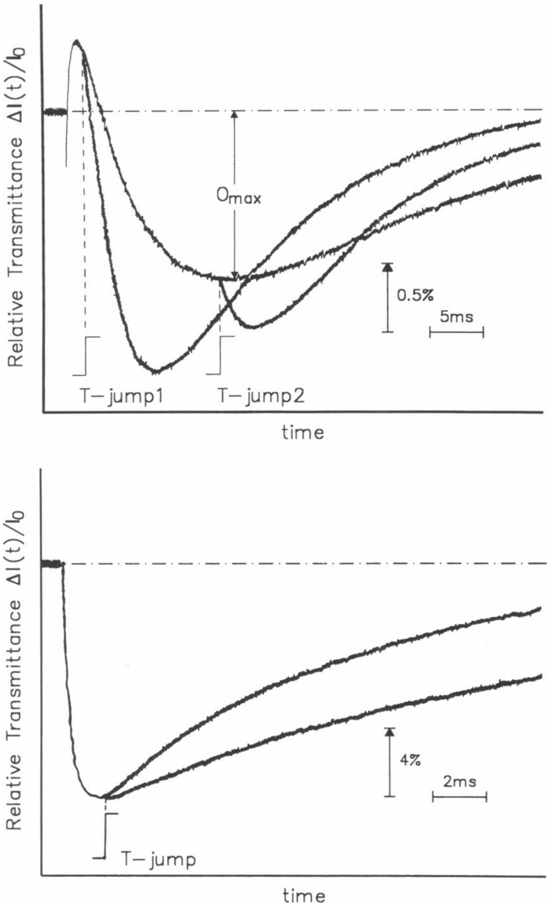

FIGURE 1 Experimental kinetic curves of formation and decay of O_{640} (*a*) (*top*) and decay of M_{410} (*b*) (*bottom*) intermediates of the bR photocycle. The unperturbed kinetic is combined with relaxation curves after T-jump(s). An accelerated decay kinetic of the M_{410} intermediate (*b*) shows the absolute amplitude of the T-jump. Initial temperature 10°C ($\tau_{1/2}$ = 17 ± 1 ms). The amplitude of the T-jump is 7.5 ± 0.7°C ($\tau_{1/2}$ = 7 ± 0.5 ms).

tional T-jump pulses at two different states of the photocycle.

Variation of pH from 4 to 10 and of temperature from 4 to 60°C led to a characteristic relationship between the maximal transient concentration of O_{640} at different pH values as given in Fig. 2. The curves have a characteristic sigmoidal shape, which was already observed for pH 7 by Sherman et al. (7) and Hoffmann et al. (23). The results in Fig. 2 show that the sigmoidal shape of the temperature dependence of the transient O_{640} concentration does not change in the studied pH range (from pH 4 to 10). The midpoints of the sigmoidal curves shift with increasing pH to higher temperatures. At pH 4 the midpoint is at ~ 15°C; at pH 9, at 55°C. From this observation it follows that at pH 10 and room temperature the concentration of O_{640} is practically negligible. However, with an increase in the temperature above 40–50°C, the O_{640} intermediate can again be detected. It should be noted that the shape of the sigmoidal curve at pH 10 (*curve 5*) is altered, which might indicate a slightly different mechanism of the photocycle (see below). The experiments using T-jump perturbation of the M_{410} and O_{640} intermediates at different pHs (e.g., pH 7 in Fig. 1, *a* and *b*) mainly confirm the dependence of the O_{640} concentration measured at stationary temperatures.

A sigmoidal behavior can be explained by a change in the concentration C of a product (here O_{640}) in equilibrium with its precursor (here N_{550}). The normalized concentrations (C_{exp}) observed experimentally can be described by the Van't Hoff equation

$$\frac{C_{exp}}{C_{sat} - C_{exp}} = f(T). \qquad (1)$$

Such an evaluation of the data provides the thermodynamic parameters of the dynamic equilibrium given here.

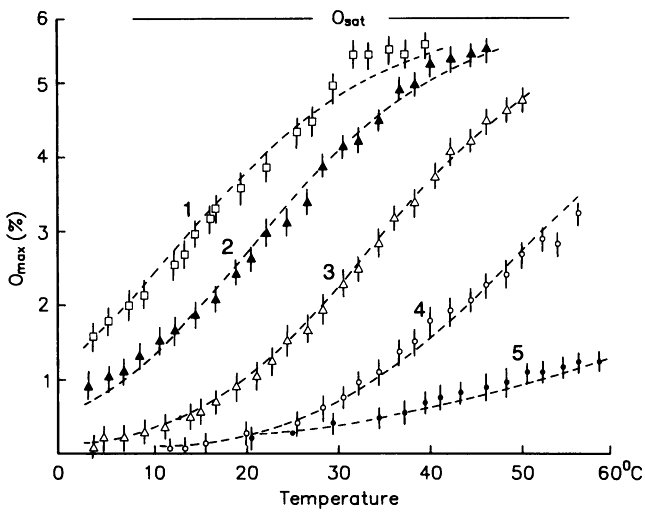

FIGURE 2 The temperature dependence of the transient concentration of the O_{640} intermediate at different pH. Differential transmittance, as measured in Fig. 1 *a*, reflects the change in concentration of O_{640}. Curves 1, 2, 3, 4, and 5 are measured at pH 4.0, 7.0, 8.0, 9.0, and 10.0, respectively. The dashed lines represent the best fit by a least-square method (see Fig. 3). The data points for pH 5.0 and 6.0 are omitted for clarity.

The sigmoidal curves for the O_{640} intermediate were first explained in the Van't Hoff formalism by Hoffmann et al. (23). The authors concluded that a conformational transition of bR exists at ambient temperature, and therefore two different pools of bR molecules must undergo photocycles with or without the O_{640} intermediate. Their model is kinetically identical to the model of Sherman et al. (7). Hoffmann et al. (23) calculated for these two conformational states a difference in enthalpy of 69.9 ± 9.7 kJ/mol. In a subsequent paper (24) the authors provided further data from spin label studies of the lipid mobility in the purple membrane sheets, which they interpreted as evidence for the existence of two bR conformers. An interpretation of the observed temperature dependence of the O_{640} intermediate as an indicator of two different species of bR in the ground state seems plausible in the case of a thermally induced exchange between two stationary states of the macromolecule. However, no further experiments confirming the proposed conformational transition in bR can be found in the literature. Moreover, calorimetric measurements of the purple membrane in the temperature range from 0 to 70°C did not detect any endothermic transition of the ground state of bR (25). This lack of data for a conformational change in the ground state implies that the two species of bR (if they exist) are distinguishable only on the basis of the spectral properties of the O_{640} intermediate, being identical (at least spectrally) in all other transient states of bR as well as in the original resting state.

There is another explanation for the sigmoidal behavior of the transient concentration of the O_{640} intermediate that is in agreement with most recently published models. In these models, for the multistep relaxation process of the $M_{410} \rightarrow$ bR reaction, a fast quasiequilibrium between at least two intermediates is assumed. Such an equilibrium is obtained if the rate constants of the forward and back reactions are large compared with either the preceding or following steps. Also, branching at a certain stage of the photocycle may be a solution of the problem (see also reference 26). In these two cases the values calculated from the Van't Hoff equation correspond to differences in the thermodynamic characteristics of the competing (case of a branching) or the quasiequilibrating (case of reversible steps) intermediates. The present data are congruent with an unbranched model as, for example, the one introduced in reference 13. In this kinetic scheme the O_{640} intermediate is coexisting in fast quasiequilibrium with the N_{550} intermediate: ... $M_{410} \Leftrightarrow [N_{550} \Leftrightarrow O_{640}] \rightarrow$ bR, where square brackets indicate that forward (k_{NO}) and back reactions (k_{ON}) $\gg k_{MN}, k_{NM}, k_{ObR}$. With increasing temperature this quasiequilibrium is shifted in favor of the O_{640} intermediate, in accord with the temperature dependency of its spectrum (13).

The thermal equilibrium between these states is determined by the ratio of the rate constants k_{NO} and k_{ON}, and the normalized concentration (W_o) of O_{640} will be

$$W_o = \frac{k_{NO}}{k_{NO} + k_{ON}} = \frac{1}{1 + \exp(-\Delta S_{ON}/R)\exp(+\Delta E_{ON}/RT)}, \quad (2)$$

where R is the universal gas constant and T the absolute temperature. $\Delta E_{ON} = E_O - E_N$ is the difference in enthalpy and $\Delta S_{ON} = S_O - S_N$ the difference in entropy between the O_{640} and the N_{550} intermediates.

The concentration will have sigmoidal dependence on the temperature. Note that the midpoint of the sigmoid, $Tm = \Delta E_{ON}/\Delta S_{ON}$, depicts the temperature at which the concentrations of states N_{550} and O_{640} are equal. A Van't Hoff representation of the data (Fig. 3) permits the determination of the differences between the enthalpy and entropy of the N_{550} and O_{640} intermediates of the bR photocycle. The least-square estimates of the data in Fig. 3 provide the following results:

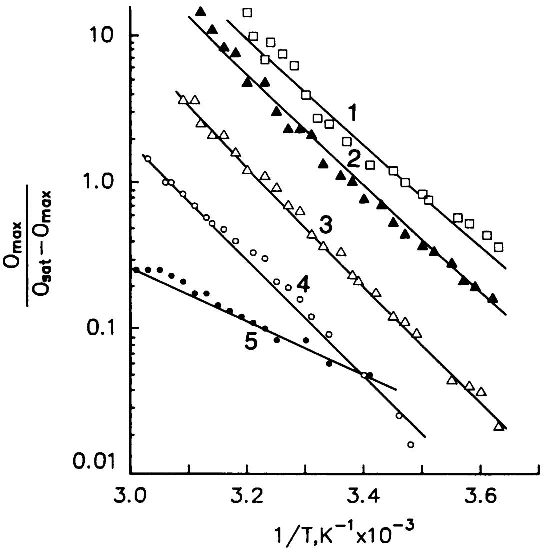

FIGURE 3 The Van't Hoff plot of the experimental points from Fig. 2. Data are fitted by the function $W_o/(1 - W_o) = \exp(-\Delta E_{ON}/RT) + \exp(+\Delta S_{ON}/R)$.

TABLE 1 Enthalpy and entropy differences between the O_{640} and N_{550} intermediate

pH	ΔE_{ON}	ΔS_{ON}	$\Delta E'_{ON}$	$\Delta S'_{ON}$
	kJ/mol	*J/mol K*	*kJ/mol*	*J/mol K*
4.0	63.3 ± 4.2	231.0 ± 12.6	73.2	273
7.0	72.4 ± 2.1	247.8 ± 8.4	74.9	264.6
8.0	77.8 ± 0.8	256.2 ± 4.2	77.8	256.2
9.0	74.9 ± 2.1	235.2 ± 8.4	81.6	243.6
10.0	35.6 ± 2.1	96.6 ± 4.2	85.8	235.2

$\Delta E'_{ON}$ and $\Delta S'_{ON}$ denote the enthalpy and entropy differences using ΔS_{ON} = 256.2 J/mol K and ΔE_{ON} = 77.8 kJ/mol, respectively. The errors were calculated by means of a standard least-square deviation procedure.

As shown in Fig. 2, the temperature of the $N_{550} \Leftrightarrow O_{640}$ transition increases with increasing pH. The relative shifts of the absolute temperature are small (3–6%). The calculated values of ΔE_{ON} and ΔS_{ON} (Table 1) are also within the range of errors independent of pH with the only exception at pH 10.0. However, some indications for a variation of these values are seen in Table 1: entropy and enthalpy are maximal near physiological pH. To estimate possible variations of ΔE_{ON} and ΔS_{ON} in the given pH range, they were fixed at 77.8 kJ/mol and 256.2 J/mol K, respectively (the values from the best fit at pH 8.0; the errors are minimal at pH 8.0 because both branches of the sigmoid are observable in the given temperature range). The experimental data can be satisfactorily described by the variation of E'_{ON} (the fourth column of Table 1) and S'_{ON} (fifth column of Table 1).

From this analysis it can be concluded that the thermodynamic characteristics of the observed transitions correlate well with a preserved underlying mechanism, at least in the pH range between 4.0 and 9.0. Therefore, a branching mechanism is improbable. In addition, it should be noted that, in spite of a very large difference in the concentration of hydrogen ions, the thermodynamic properties of the observed transition are not strongly affected. In other words, the functional center of the bR molecule is perfectly shielded against such a large pH gradient. This is in agreement with the observation that internal Asp residues are not deprotonated even at high pH values (27; Metz, G., F. Siebert, and M. Engelhard, unpublished data).

At pH 10.0 the shape of the sigmoidal curvature appears to be broader, the slope of the Van't Hoff plot flatter (Figs. 2 and 3), and the calculated entropy and enthalpy changes decreased (Table 1). The following two reasons might explain this effect. At high pH the condition of quasiequilibrium between N_{550} and O_{640} states might be disturbed. In this case the usage of an equilibrium constant is incorrect. Secondly, with increasing pH the temperature of the transition, *Tm*, is shifted to higher values and might overlap with a reversible thermal denaturation of bR (28), causing the Van't Hoff equation to be inapplicable.

The calculated values for the enthalpy and entropy changes of the $N_{550} \Leftrightarrow O_{640}$ transition are typical for conformational transitions in proteins and are well in agreement with the results published in reference 29. The entropy difference ΔS_{ON} of ~252 J/mol K can be caused from, for example, ~10–20 bonds in the protein (including also hydrogen and van der Waals bonds) that will acquire rotational degrees of freedom during the transformation of bR from N_{550} to O_{640}. This number is bigger than those that are capable of such transformations and that are in the close neighborhood of the retinal (because this transition induces a spectral change of the chromophore). On the other hand, this amount is less than the total number of groups in bR capable of such transitions. In fact, a relatively small number of thermalized groups (groups that acquire additional degrees of freedom) in a protein gives the significant change of the functional state.[1]

In summary, it might be suggested that the O_{640} intermediate is disordered in comparison to N_{550} and that some peripheral amino acid side chains of bR also have to be involved in the $N_{550} \rightarrow O_{640}$ process.

The excellent technical assistance of H. Ristau and the typing of the manuscript by C. Riemer are gratefully acknowledged.

Dedicated to K. Schaffner on the occasion of his 60th birthday.

Received for publication 8 July 1991 and in final form 4 November 1991.

REFERENCES

1. Hess, B., D. Kuschmitz, and M. Engelhard. 1982. Bacteriorhodopsin. *In* Membranes and Transport 2. A. N. Martonosi, editor. Plenum Press, New York. 309–318.
2. Stoeckenius, W., and R. A. Bogomolni. 1982. Bacteriorhodopsin and related pigments of halobacteria. *Annu. Rev. Biochem.* 52:587–616.
3. Ovchinnikov, Y. A., N. G. Abdulaev, and N. N. Modyanov. 1982. Structural basis of proton translocating protein function. *Annu. Rev. Biophys.* 11:445–463.
4. Oesterhelt, D., and J. Tittor. 1989. Two pumps one principle: light-driven ion transport in Halobacteria. *Trends Biochem. Sci.* 14:57–61.
5. Chu Kung, M., D. DeVault, B. Hess, and D. Oesterhelt. 1975. Photolysis of bacterial rhodopsin. *Biophys. J.* 15:907–911.
6. Lozier, R. H., R. A. Bogomolni, and W. Stoeckenius. 1975. Bacteriorhodopsin: a light driven proton pump in *Halobacterium halobium. Biophys. J.* 15:955–962.
7. Sherman, W. V., R. R. Eicke, S. R. Stafford, and F. M. Wasacz. 1979. Branching in the bacteriorhodopsin photochemical cycle. *Photochem. Photobiol.* 30:727–729.
8. Lozier, R. H., W. Niederberger, R. A. Bogomolni, S. B. Hwang, and W. Stoeckenius. 1976. Kinetics and stoichiometry of light-induced proton release and uptake from purple membrane fragments, *Halobacterium halobium* cell envelopes, and phospholipid vesicles containing oriented purple membrane. *Biochim. Biophys. Acta.* 440:545–556.
9. Eisenbach, M., E. P. Bakker, R. Korenstein, and S. R. Caplan. 1976. Bacteriorhodopsin biphasic kinetics of phototransients and of light-induced proton transfer by sub-bacterial particles and liposomes. *FEBS (Fed. Eur. Biochem. Soc.) Lett.* 71:228–232.
10. R. Korenstein, B. Hess, and D. Kuschmitz. 1978. Branching reactions in the photocycle of bacteriorhodopsin. *FEBS (Fed. Eur. Biochem. Soc.) Lett.* 93:266–270.
11. Groma, G. I., and Z. S. Dancshazy. 1986. How many M forms are there in the bacteriorhodopsin photocycle? *Biophys. J.* 50:357–366.
12. Parodi, L. A., R. H. Lozier, S. M. Bhattacharjee, and J. F. Nagle. 1984. Testing kinetic models for the bacteriorhodopsin photocycle. II. Inclusion of an O to M backreaction. *Photochem. Photobiol.* 40:501–512.
13. Chernavskii, D. S., I. V. Chizhov, R. H. Lozier, T. M. Murina, A. M. Prokhorov, and B. V. Zubov. 1989. Kinetic model of bacteriorhodopsin photocycle: pathway from M state to bR. *Photochem. Photobiol.* 49:649–653.
14. Dancshazy, Z., Govindjee, R., Nelson, B., and Ebrey, T. G. 1986. A new intermediate in the photocycle of bacteriorhodopsin. *FEBS (Fed. Eur. Biochem. Soc.) Lett.* 209:44–48.
15. Drachev, L. A., A. D. Kaulen, V. P. Skulachev, and V. V. Zorina. 1986. Protonation of a novel intermediate P is involved in the M → br step of the bacteriorhodopsin photocycle. *FEBS (Fed. Eur. Biochem. Soc.) Lett.* 209:316–320.
16. Kouyama, T., A. N. Kouyama, A. Ikegami, M. K. Mathew, and W. Stoeckenius. 1988. The bacteriorhodopsin photoreactions: identification of a long-lived intermediate, N (P, R350), at high pH and its M-like photoproduct. *Biochemistry.* 27:5855–5863.
17. Fodor, S. P. A., J. B. Ames, R. Gebhard, E. M. M. Van den Berg, W. Stoeckenius, J. Lugtenburg, and R. A. Mathies. 1988. Chromophore structure in bacteriorhodopsin's N intermediate: implications for the proton-pumping mechanism. *Biochemistry.* 27:7097–7101.
18. Váró, G., and K. Lanyi. 1990. Pathways of the rise and decay of the M photointermediate(s) of bacteriorhodopsin. *Biochemistry.* 29:2241–2250.
19. Ames, J. B., and R. A. Mathies. 1990. The role of back-reactions and proton uptake during the N → O transition in bacteriorhodopsin's photocycle: a kinetic resonance Raman study. *Biochemistry.* 29:7181–7190.
20. Oesterhelt, D., and W. Stoeckenius. 1974. Isolation of the cell membrane of *Halobacterium halobium* and its fractionation into red and purple membrane. *Methods Enzymol.* 31:667–678.

---

[1] This is not unusual if a protein is considered as a construction created for a specific function. Indeed, only in this case can the "melting" of a small but functionally significant zone of the macromolecule provide the change of state of the construction at all. The theoretical background of this so-called "protein-engine" concept has been discussed in reference 30.

21. Tsuji, K., and B. Hess. 1986. Electric-field induced conformational changes of bacteriorhodopsin in purple membrane films. *Eur. Biophys. J.* 13:273–280.

22. Bernasconi, C. F. 1976. Relaxation Kinetics. Academic Press, New York. p. 288.

23. Hoffmann, W., M. Graca-Miguel, P. Barnard, and D. Chapman. 1978. Evidence for conformational transitions in bacteriorhodopsin. *FEBS (Fed. Eur. Biochem. Soc.) Lett.* 95:31–34.

24. Hoffmann, W., A. D. Clark, M. Turner, S. Wyard, and D. Chapman. 1980. Bacteriorhodopsin, boundary lipid and protein conformers: a spin label study. *Biochim. Biophys. Acta.* 598:178–183.

25. Jackson, M. B., and J. M. Sturtevant. 1978. Phase transitions of the purple membranes of *Halobacterium halobium. Biochemistry.* 17:911–915.

26. Váró, G., A. Duschl, and Janos K. Lanyi. 1990. Interconversions of the M, N, and O intermediates in the bacteriorhodopsin photocycle. *Biochemistry.* 29:3798–3804.

27. Engelhard, M., K. Gerwert, B. Hess, W. Kreutz, and F. Siebert. 1985. Light-driven protonation changes of internal aspartic acids of bacteriorhodopsin: an investigation by static and time-resolved infrared difference spectroscopy using [4-^{13}C] aspartic acid labeled purple membrane. *Biochemistry.* 24:400–407.

28. Plakunova, V. G. 1975. Reversible thermal bleaching of the purple membrane complex of bacteriorhodopsin. *Biol. Nauki* (*Mosc.*). 18:56–59.

29. Ort, D. R., and W. W. Parson. 1979. Enthalpy changes during the photochemical cycle of bacteriorhodopsin. *Biophys. J.* 25:355–364.

30. Chernavskii, D. S., Y. I. Khurgin, and S. E. Shnol. 1987. The "protein-engine" concept and its consequences. *Biofizika.* 32:775–781.